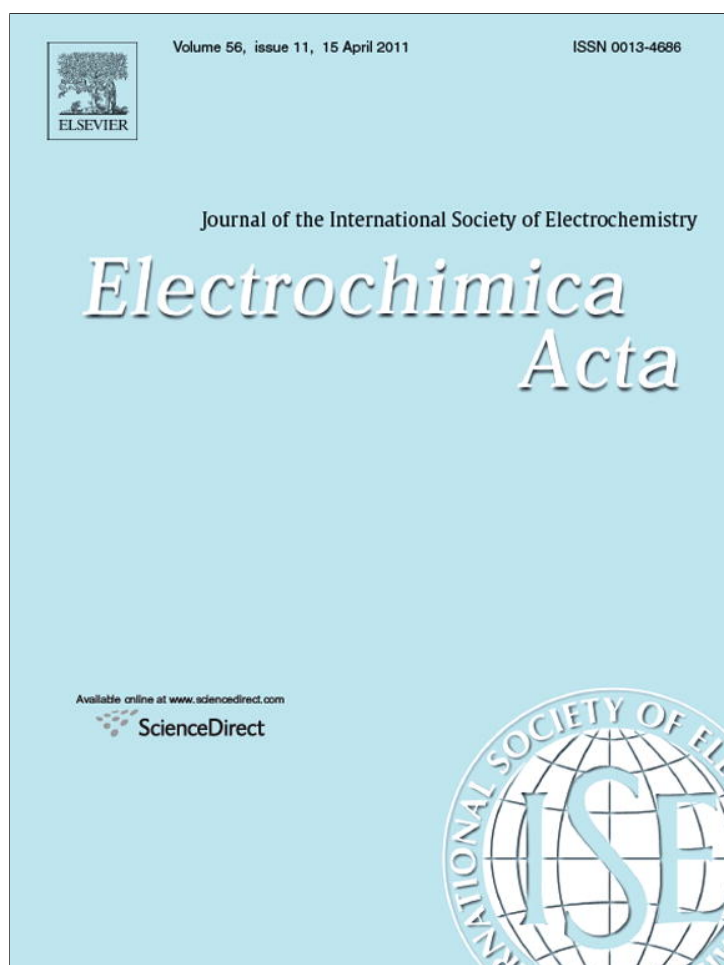


Provided for non-commercial research and education use.
Not for reproduction, distribution or commercial use.



This article appeared in a journal published by Elsevier. The attached copy is furnished to the author for internal non-commercial research and education use, including for instruction at the authors institution and sharing with colleagues.

Other uses, including reproduction and distribution, or selling or licensing copies, or posting to personal, institutional or third party websites are prohibited.

In most cases authors are permitted to post their version of the article (e.g. in Word or Tex form) to their personal website or institutional repository. Authors requiring further information regarding Elsevier's archiving and manuscript policies are encouraged to visit:

<http://www.elsevier.com/copyright>



Electrochemical deposition of zinc oxide on a thin nickel buffer layer on silicon substrates

E.B. Chubenko^{a,*}, A.A. Klyshko^a, V.P. Bondarenko^a, M. Balucani^b

^a Department of Micro & Nanoelectronics, Belarusian State University of Informatics and Radioelectronics, P. Brovki str, 6, Minsk 220013, Belarus

^b Electronics Engineering Department, University of Rome "La Sapienza", Rome 00184, Italy

ARTICLE INFO

Article history:

Received 7 September 2010

Received in revised form 1 February 2011

Accepted 2 February 2011

Available online 2 March 2011

Keywords:

Electrochemical deposition

Zinc oxide

Porous silicon

Voltammetry

Scanning electron microscopy

ABSTRACT

Electrochemical deposition of ZnO from aqueous nitrate solutions on nickel and platinum electrodes was investigated using the voltammetry technique to determine the optimal regimes in both potentiostatic and galvanostatic modes for acquiring polycrystalline ZnO films. Scanning electron microscopy, X-ray diffractometry, and X-ray microanalysis of the formed ZnO films are presented, showing a polycrystalline structure of the ZnO films with a preferable orientation in the (0002) direction and an exact stoichiometric composition. The deposited ZnO films demonstrate a strong visible yellow-greenish photoluminescence at room temperature with a maximum at 600 nm that can be referred to crystal lattice oxygen defects. The maximum of the photoluminescence excitation spectrum at 370 nm corresponds to the band gap of ZnO (3.3–3.35 eV) confirming that band-to-band excitation mechanism takes place.

© 2011 Elsevier Ltd. All rights reserved.

1. Introduction

Nowadays, zinc oxide (ZnO) is recognized as a promising material for optoelectronic, photovoltaic, sensing, and piezoelectric devices [1–3]. The main problem to be solved for industrial application of ZnO is unavailability of large-sized ZnO substrates workable with modern manufacturing equipment [4]. The development of large-sized silicon substrates covered with ZnO film can be a feasible solution. Furthermore, the availability of ZnO on silicon wafers will promote the direct integration of ZnO-based devices with CMOS silicon integrated circuit technology. However direct ZnO deposition on the surface of the silicon substrate is a challenge due to different types of crystal lattices and a difference in coefficients of thermal expansion ($\alpha_a = 6.51 \mu\text{m m}^{-1} \text{K}^{-1}$ and $\alpha_c = 3.02 \mu\text{m m}^{-1} \text{K}^{-1}$ for the different crystallographic orientations of ZnO and $\alpha = 2.6 \mu\text{m m}^{-1} \text{K}^{-1}$ for Si) [5,6]. To reduce the effect of these differences, buffer layers can be used to lower the stress between the substrate and the deposited ZnO film. Porous silicon can be used as such the buffer layer, as was illustrated by the deposition of GaAs [7], metal chalcogenides [8–10], and diamond [11] films.

Similar to other metal oxides, ZnO films can be formed by the electrochemical technique. In comparison with the epitaxy, this technique allows reducing of a thermal budget in the production of

semiconductor devices, is lower in cost, and enables a simultaneous processing of large surfaces of composite pattern [3]. The ZnO film structure formed is easily controlled by varying the electrochemical deposition process regimes.

When the zinc oxide is deposited from aqueous electrolytes at 70–85 °C directly on porous silicon, the formation of hydroxide ions at the electrode space [12] may lead to oxidation and destruction of porous silicon [13]. The use of a thin nickel sublayer to protect porous silicon and to improve the current distribution over the substrate surface during ZnO deposition is discussed in the present work. The nickel layer may also be used as a bottom contact in the integrated devices based on zinc oxide.

2. Experimental

For the ZnO electrochemical deposition an aqueous solution containing 0.05–0.1 M of $\text{Zn}(\text{NO}_3)_2$ was used. The electrochemical bath was prepared by mixing of calculated quantities of ZnO and HNO_3 of analytical grade quality in distilled water.

The ZnO electrochemical deposition process was studied by the cyclic voltammetry technique. A three-electrode glass electrochemical cell with a magnetic stirrer and temperature control was used. A standard commercial Ag/AgCl electrode and platinum grid were used, respectively, as the reference electrode and as the counter electrode. A potential scanning was performed with the PI-50-1.1 potentiogalvanostat controlled by the Advantech PCI-1710HG board.

* Corresponding author. Tel.: +375 17 2938843.

E-mail address: eugene.chubenko@gmail.com (E.B. Chubenko).

Voltammetry measurements were carried out on the platinum (Pt) and nickel (Ni) electrodes. Prior to the experiments, Pt electrodes were sequentially processed under anodic and cathodic polarization in 0.05 M H₂SO₄ solution for 30 min at 15 mA/cm² current density. Such treatment removes any impurities from the Pt electrode surface to make it reproducible. The Ni electrodes were cleaned in acetone followed by bright etching for 10 s in the solution containing 85 ml of H₃PO₄ and 15 ml of HNO₃ at 100 °C. Then Ni electrodes were rinsed in distilled water and treated in 0.05 M H₂SO₄ solution, as was done for the Pt electrodes. Reproducibility of the Pt and Ni electrodes was controlled by the checking of the equilibrium potential in the electrochemical bath.

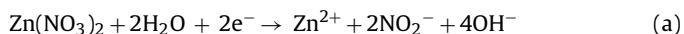
ZnO films were deposited on n⁺-type antimony doped Si (1 1 1) substrates (0.01 Ω × cm) with porous silicon buffer layer covered with Ni layer. Prior to the Ni deposition, the Si substrates were immersed in the 4.5% HF solution to remove a native SiO₂ layer. To form porous silicon layer Si substrates were anodized for 20 s in the HF solution of HF:H₂O:C₃H₇OH = 1:3:1 composition at current density of 80 mA/cm². The thin (0.8 μm) porous silicon layer formed drastically increases the adhesion and reduces mechanical stresses of the metal and the semiconductor films deposited on top of it later. The thin Ni layer, up to 100 nm in thickness, was electrochemically deposited onto the PS layer from an industrial sulfamic solution.

The surface morphology and composition of the electrochemically deposited ZnO films were studied with the Hitachi S-4800 scanning electron microscope operating at 15 kV. The phase composition was studied by the X-ray diffractometry (XRD) with DRON-3 apparatus (RPE "Bourevestnik" Inc., Russia) using the CuKα source. The photoluminescence spectra of ZnO were measured at room temperature (20 °C) with LOMO MDR-23 monochromator and the FEU-100 photomultiplier in photon counting mode as a detector. The 500 W Xe lamp served as an excitation light source. The LOMO MDR-12 monochromator was used to cut out monochromatic lines from the spectrum of the Xe lamp.

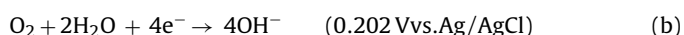
3. Results and discussions

3.1. Voltammetry of the ZnO deposition

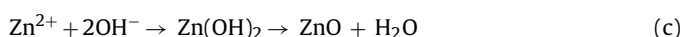
The zinc oxide electrochemical deposition is a two-stage process [12]. At the first stage, nitrate ions with the participation of electrons transform into the nitrite ions with the formation of the hydroxyl ions:



The standard electrode potential of this reaction relative to the Ag/AgCl reference electrode is equal to −0.189 V. Since soluted oxygen is present in the electrolyte, either being specially introduced or from air, the following electrochemical reaction can take place resulting in the formation of the hydroxyl ions as well [14]:



Accumulation of the large amount of the hydroxyl ions locally increases pH at the cathode space. In alkaline solution, the presence of zinc hydroxide phase is possible. Zn(OH)₂ can decompose spontaneously to form ZnO. So, the second stage of the zinc oxide deposition can be described by the two-step chemical reaction:



As follows from the above expressions, the process of the ZnO electrochemical deposition should take place at the potentials close to zero. However, ZnO deposition is observed only at potentials below −0.7 V. According to Ref. [12], a small value of the constant of the reaction rate and low diffusion rates of reagents result in a considerable overvoltage of the deposition of semiconductor compound.

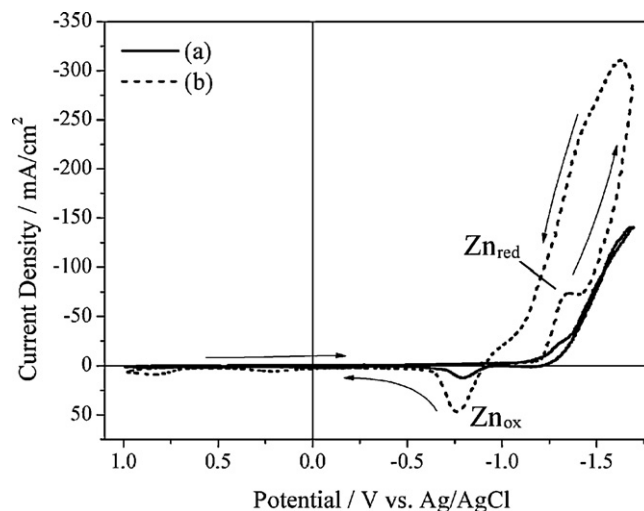


Fig. 1. Cyclic voltammograms of the Pt electrode in the aqueous solutions containing (a) 0.05 M Zn²⁺, 0.2 M NO₃⁻ and (b) 0.1 M Zn²⁺, 0.2 M NO₃⁻ (i.e. 0.1 M Zn(NO₃)₂) at 60 °C; the first scan; pH = 5.4. The scan rate is 100 mV/s.

Moreover, to reduce the nitrate ions, adsorbed Zn²⁺ cations acting as catalyst are required on the cathode surface. For this reason, the ZnO deposition potential shifts to the range of the Zn deposition potentials, i.e. de facto the process is considered as the underpotential deposition.

An analysis of voltammograms of the platinum electrode in the zinc nitrate solution showed that the first cycle of the cyclic potential scanning differs from the subsequent ones. Fig. 1 presents the first cycle of voltammograms of the platinum electrode in aqueous solutions containing 0.1 M Zn²⁺ and 0.05 M Zn²⁺ with the same 0.2 M concentration of NO₃⁻ ions at 60 °C and pH = 5.4.

The pronounced current density peak at the cathode polarization in the range of −1.3 V corresponds to the metallic zinc deposition by the reaction:



At the anode polarization around −0.8 V, the current peak associated with the dissolution of the metal deposited at the cathode polarization is observed. The change in the concentration of the Zn²⁺ ions resulted in the proportional change in the intensities of zinc deposition and dissolution peaks. The current increase at the potentials above −1.3 V is conditioned by hydrogen evolving at the cathode due to the direct water electrolysis.

Behavior of the current during second and all subsequent potential scans was the same but different from that observed during the first cycle. Fig. 2 shows the second cycle of voltammograms of the platinum electrode in the above mentioned solutions. The current peak near −1 V and a small plateau at a less potential value are observed in the curves at the cathode polarization. Similar behavior of the current in the cyclic voltammograms is observed for the deposition of other metal chalcogenides from aqueous electrolytes [10]. This range corresponds to the deposition of the ZnO binary compound via the Zn²⁺ ions adsorbed at the cathode surface [12].

The change in the zinc ions concentration in the electrolyte resulted in a considerable increase of the cathode current during the second cycle of the voltammograms, emphasizing an important role of the zinc ions in the reduction of nitrate ions.

Referring to Fig. 2, two peaks are observed in the voltammograms at the anode polarization. The first peak located at −0.8 V is associated with the dissolution of metallic zinc. The second peak located at near −0.6 V is probably related to the dissolution of zinc oxide. It should be noted that during voltammograms recording, the value of these peaks constantly decreased. Presumably, at every

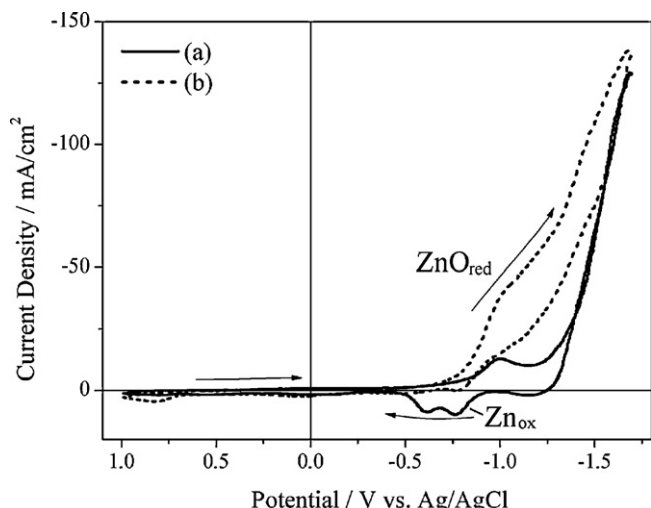


Fig. 2. Cyclic voltammograms of the Pt electrode in the aqueous solution containing (a) 0.05 M Zn^{2+} , 0.2 M NO_3^- and (b) 0.1 M Zn^{2+} , 0.2 M NO_3^- (i.e. 0.1 M $Zn(NO_3)_2$) at 60 °C; the second scan; pH = 5.4. The scan rate is 100 mV/s.

step of the cathode polarization the electrode surface has been covering with the deposit of certain thickness and resistance, which was not dissolved completely during the anode polarization, i.e. the reaction of ZnO deposition from the considered aqueous $Zn(NO_3)_2$ solution is not completely reversible.

Referring to Fig. 3, the rate of the zinc oxide precipitation at the cathode also depends on the electrolyte temperature. The peaks in the range of -1.3 V at the cathode polarization and in the range of -0.8 V at the anode polarization are associated with the deposition and dissolution of metallic zinc and they are both well observed at the electrolyte temperature of 20 °C and 40 °C. The process of the ZnO deposition predominates at higher electrolyte temperatures.

Voltammograms of the nickel electrodes were qualitatively the same as discussed above of platinum electrodes. Fig. 4 shows the second cycle of the voltammograms of the nickel electrode in 0.1 M $Zn(NO_3)_2$ solution at different electrolyte temperatures. As shown in Fig. 4, the peak related to the metal Zn deposition is more prominent in the curve recorded at the lower electrolyte temperatures, while the peak corresponding to the ZnO deposition is pronounced at -1 V in the curves recorded at 60 °C and 80 °C.

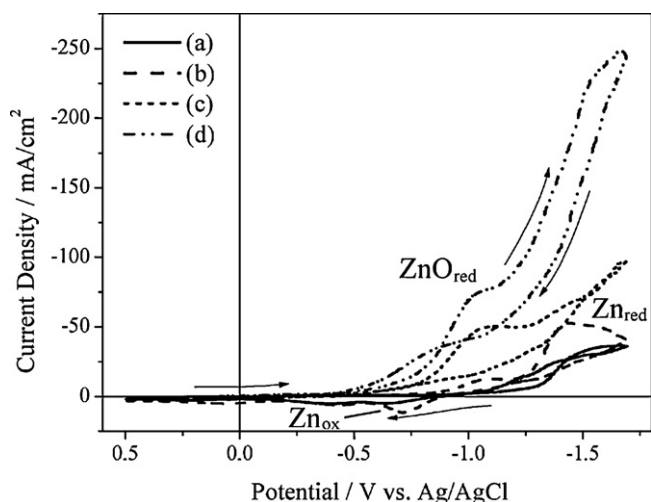


Fig. 3. Cyclic voltammograms of the Pt electrode in the aqueous 0.1 M $Zn(NO_3)_2$ solution at different electrolyte temperatures: (a) 20 °C, (b) 40 °C, (c) 60 °C, and (d) 80 °C; the second scan. pH of the solution decreases from 5.8 at 20 °C to 5.2 at 80 °C. The scan rate is 100 mV/s.

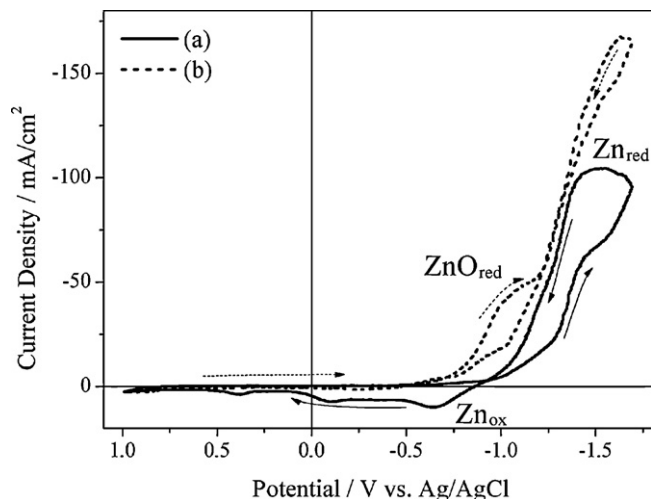


Fig. 4. Cyclic voltammograms of the Ni electrode in the aqueous solution containing 0.1 M $Zn(NO_3)_2$ at different electrolyte temperatures: (a) 20 °C and (b) 60 °C. The second scan; the scan rate is 100 mV/s.

The recorded voltammograms allow to determine the parameters of the potentiostatic mode of zinc oxide deposition on the platinum and nickel electrodes. For both electrode types, the zinc oxide deposition takes place in the range from -0.8 V to -1.1 V vs. the Ag/AgCl reference electrode with the optimal electrolyte temperature between 60 °C and 80 °C. The potentiostatic mode (i.e. at the constant potential) allows controlling the state of the electrode/electrolyte interface and the composition of the deposit. However, the galvanostatic mode (i.e. at the constant current density) providing an easy control of deposition rate, deposit thickness, is much more practically feasible and it can be realized in the simple two-electrode cell.

In order to switch to the galvanostatic mode, the current density for the ZnO deposition was specified equal to that during the steady-state growth under potentiostatic conditions. It was found to be in the range from 2 to 10 mA/cm². Fig. 5 shows the variation of the potential during the ZnO electrochemical deposition in the galvanostatic mode on the silicon/porous silicon/nickel substrates from the aqueous 0.05 M $Zn(NO_3)_2$ solution at 70 °C at different current densities. The electric contact was made directly to the nickel layer. As can be seen from Fig. 5, the curve behavior is the same for

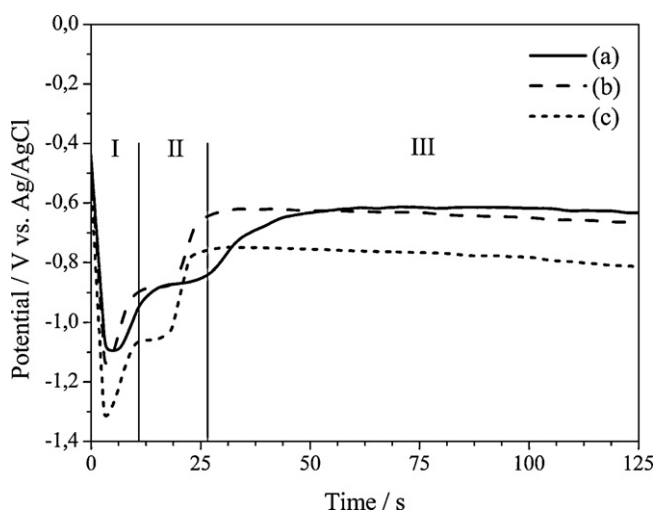


Fig. 5. The variation of the potential during the ZnO electrochemical deposition in the galvanostatic mode from the aqueous 0.05 M $Zn(NO_3)_2$ solution at the 70 °C electrolyte temperature (pH = 5.5) at: (a) 2.5 mA/cm², (b) 5 mA/cm², (c) 7 mA/cm².

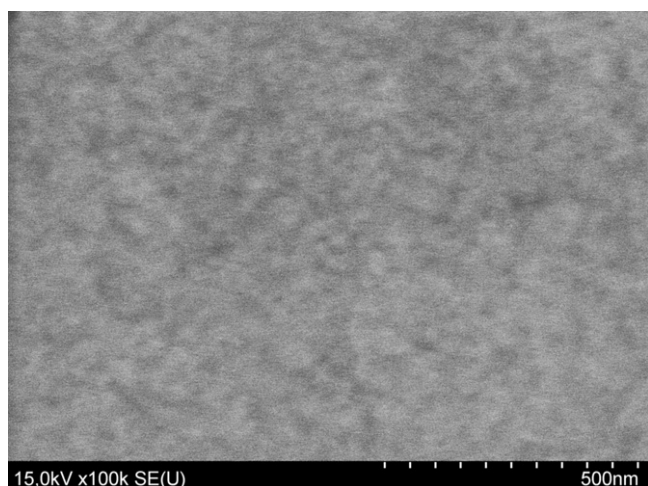


Fig. 6. The plan view SEM micrograph of the Ni layer deposited on the n+ porous silicon substrate from the conventional commercial sulfamic solution.

all current densities used. At higher current densities the hydrogen evolving due to direct water electrolysis deteriorates the uniformity of the film deposited. Referring to Fig. 5, several characteristic regions can be distinguished in such curves.

The potential behavior in the regions I and II is conditioned by the processes of the formation and growth of the initial film that may predominantly consist of zinc. This can be partially explained considering the first measured cycle of the voltammograms that shows that only zinc is deposited in the early stage of the process. However, real effects responsible for the potential behavior in the region II are still to be understood and are the subject of further studies.

The potential behavior in the region III is conditioned by the process of the steady-state growth of the zinc oxide film. The potential in this region is exactly in the range of the zinc oxide deposition potentials measured from the voltammograms. The gradual increase of potential absolute value with the process time is dictated by the increase in the thickness of the deposited intrinsic ZnO wide-gap semiconductor of high resistance.

3.2. The structure and composition of ZnO deposits

The structure of the zinc oxide films deposited electrochemically on the silicon/porous silicon/nickel substrates in the galvanostatic mode from the aqueous 0.05 M $\text{Zn}(\text{NO}_3)_2$ solution at the electrolyte temperature of 70 °C (pH = 5.5) was studied by the scanning electron microscopy (SEM). Fig. 6 presents a plan view of the Ni layer surface on which the ZnO deposition was performed. As one can see, the surface of Ni layer is uniform and smooth.

The thickness of the ZnO films formed at different current densities was made equal to 6 μm . The ZnO films have good adhesion to the substrate and high mechanical strength. Fig. 7 shows plane view SEM micrographs of the surfaces of the zinc oxide films formed at different current densities. As the current density increases, the deposit becomes more compact. So, for the 2.5 mA/cm^2 current density, the deposit consists of single crystallites, and for the 7 mA/cm^2 current density, it is a continuous film with the smooth surface and substantially smaller number of structural defects. Inset in a corner of the image (c) shows the roughness of the ZnO film. The size of single grains does not exceed 20 nm.

The elemental composition of the zinc oxide films was studied by the X-ray microanalysis. All the ZnO deposits, independently of the current densities used, contain 50 atomic percents of zinc and 50 atomic percents of oxygen (i.e. ZnO has a stoichiometric compo-

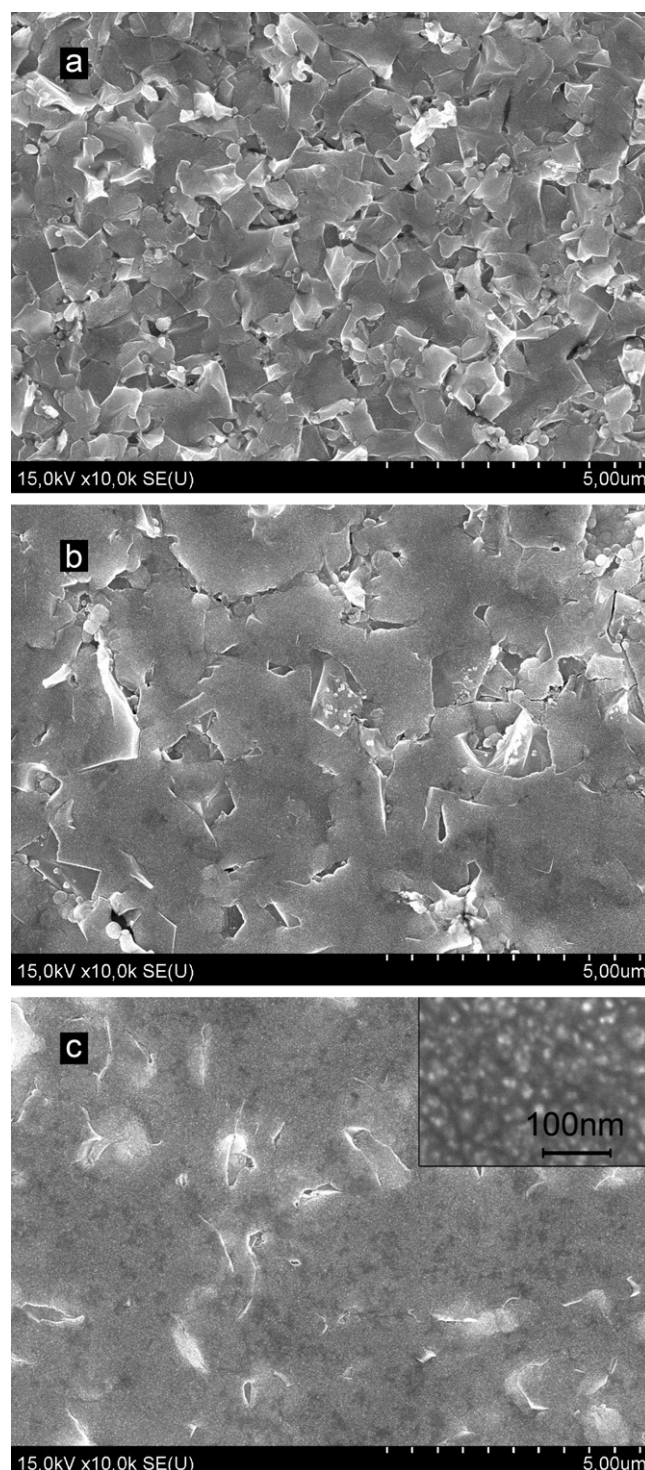


Fig. 7. SEM images of the ZnO film formed on the silicon/porous silicon/nickel substrate in the aqueous 0.05 M $\text{Zn}(\text{NO}_3)_2$ solution (pH = 5.5) at the 70 °C electrolyte temperature at different current densities: (a) 2.5 mA/cm^2 , (b) 5 mA/cm^2 , (c) 7 mA/cm^2 .

sition). Fig. 8 shows the XRD spectra of the zinc oxide films. As can be seen from Fig. 8, the films formed at any current density consist of the ZnO crystals with the preferred orientation (0002). The sample formed at 5 mA/cm^2 presents a maximum response related to this phase. So, the zinc oxide films formed can be considered as polycrystalline films.

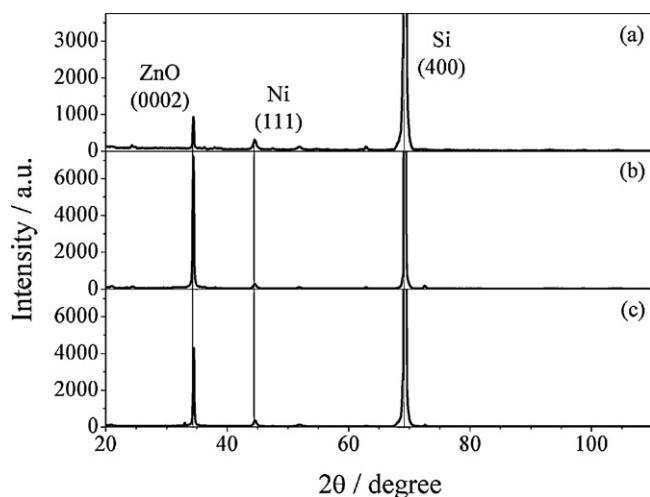


Fig. 8. XRD patterns of ZnO films deposited on the silicon/porous silicon/nickel substrate from the aqueous 0.05 M $\text{Zn}(\text{NO}_3)_2$ solution at 70 °C (pH = 5.5) at different current densities: (a) 2.5 mA/cm², (b) 5 mA/cm², (c) 7 mA/cm².

3.3. The photoluminescence of ZnO films

The same samples as for the structural studies were used for the optical investigations. The photoluminescence excitation was done at 320 nm wavelength and all the measurements were performed at room temperature (20 °C). Fig. 9 shows the photoluminescence spectra of the zinc oxide films electrochemically deposited on the silicon/porous silicon/nickel substrates. As seen from Fig. 9, the zinc oxide films demonstrate only one wide photoluminescence band with a maximum around 610 nm in the red-orange range. As the samples under study were not doped specially and were free from unintentional impurities according to the X-ray microanalysis, it is obvious that this band is due to the internal defects of material [15,16]. The sample formed at 5 mA/cm² exhibits the most intensive photoluminescence. As discussed above, this sample demonstrated the most intense peak related to the ZnO (0002) crystal phase in the XRD plot.

As shown in Refs. [15,16], the photoluminescence spectra of ZnO may consist of two independent bands, and the recombination pro-

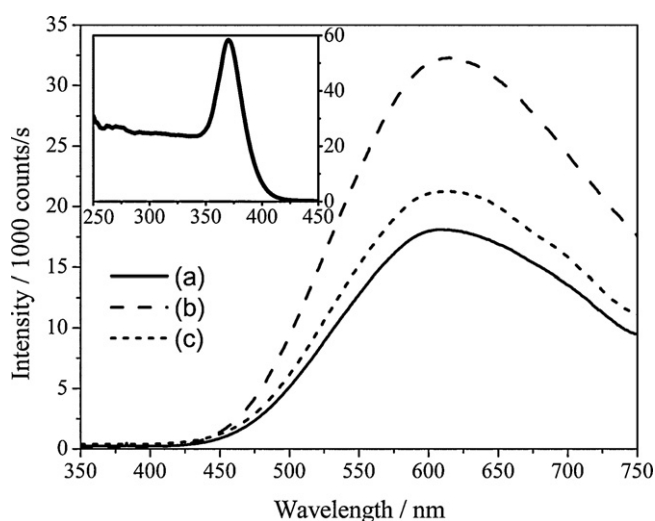


Fig. 9. Photoluminescence spectra (at 20 °C) of ZnO films deposited on the silicon/porous silicon/nickel substrates at different current densities from the aqueous 0.05 M $\text{Zn}(\text{NO}_3)_2$ solution at 70 °C with pH = 5.5: (a) 2.5 mA/cm², (b) 5 mA/cm², (c) 7 mA/cm². Inset shows photoluminescence excitation spectra (recorded at 20 °C) of the ZnO film deposited at current density 5 mA/cm².

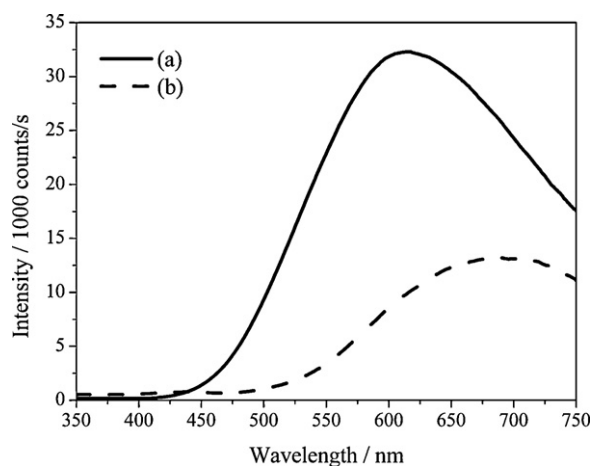


Fig. 10. Photoluminescence spectra (at 20 °C) of ZnO film deposited on the silicon/porous silicon/nickel substrates from the aqueous 0.05 M $\text{Zn}(\text{NO}_3)_2$ solution (70 °C, pH = 5.5) at 5 mA/cm²: (a) after deposition, (b) after 15 min annealing at 500 °C in air.

cesses is via the levels in the semiconductor band gap due to ionized oxygen vacancies and oxygen atoms in the interstitial sites of the ZnO crystal lattice. The photoluminescence band emitted by the oxygen vacancies has maximum in the more short-wave (550 nm) range of the spectrum, while the band emitted by the oxygen atoms in the interstitial sites has maximum at longer (650 nm) wavelength. The position and intensity of maxima can vary depending on the exciting wavelength [15] and the material structure [15,17].

Inset on Fig. 9 shows typical photoluminescence excitation spectra of the zinc oxide films discussed. The radiation was recorded at wavelength of 600 nm close to photoluminescence maximum. Maximum of the excitation spectra is at 370–375 nm, corresponding to 3.35–3.3 eV which agrees well with the value of band gap of bulk ZnO. Thus, photoluminescence excitation takes place via band-to-band mechanism.

A thermal annealing of the electrochemically deposited zinc oxide film on silicon/porous silicon/nickel substrate resulted in a decrease in the intensity and shift of the photoluminescence maximum to more long-wave range as illustrated in Fig. 10.

When the ZnO film is annealed in air, free oxygen is adsorbed at the material surface, ionized, and embedded in the ZnO crystal lattice. Hence, the most part of the oxygen vacancies is compensated, while the concentration of the oxygen atoms in the interstitial sites remains the same and even increases at the surface. These processes result in the decrease in the intensity of the photoluminescence band (at 550 nm) associated with the ionized oxygen vacancies. The intensity of the photoluminescence band due to the oxygen atoms in the interstitial sites of the ZnO crystal lattice remains the same or may slightly increase [15]. This assumption explains observed behavior of the photoluminescence spectra after thermal annealing.

4. Conclusions

Investigation of the electrochemical deposition of ZnO on platinum and nickel electrodes by cyclic voltammetry method allowed some key features of the process to be established. At the initial stage of the process only the deposition of metallic zinc takes place, which serves as the catalyst for the further formation of the compound semiconductor film. The range of the ZnO deposition potentials is actually determined by the deposition potential of metallic component, as in the case of the under-potential deposition. For the considered metal electrodes this range is from –1.1 to –0.8 V vs. Ag/AgCl electrode for temperatures from 60 to 80 °C.

It has been shown that continuous polycrystalline ZnO films can be obtained via simple and inexpensive electrochemical deposition technique on silicon/porous silicon/nickel substrates. Formed polycrystalline semiconductor films have crystallographic orientation (0002) with good adhesion to the substrate. For an electrochemical method they also demonstrate high intensity of the photoluminescence in the visible range in the region of 610 nm. Maximum of the photoluminescence excitation spectra is at 370–375 nm, which corresponds to 3.35–3.3 eV – the band gap of a bulk ZnO.

Acknowledgments

The work has been funded as a part of the Belarus Government Research Program “Crystalline and molecular structures”.

Authors would like to thank V. Tzibulsky from the “DS Belmicrossystems” subsidiary of “INTEGRAL” JSC for the SEM images preparation, L. Postnova and V. Levchenko for their assistance in the XRD studies and helpful advices. Special thanks are expressed to P. Pershukovich for the photoluminescence measurements and to V. Petrovich and V. Yakovtseva for fruitful discussions.

References

- [1] Z.L. Wang, *Mater. Today* 7 (2004) 26.
- [2] H. Ohta, H. Hosono, *Mater. Today* 7 (2004) 42.
- [3] D. Lincot, *Thin Solid Films* 487 (2005) 40.
- [4] L.N. Dem'yanets, V.I. Lyutin, *J. Cryst. Growth* 310 (2008) 993.
- [5] J. Albertsson, S.C. Abrahams, A. Kvick, *Acta Crystallogr. Sect. B: Struct. Sci.* 45 (1989) 34.
- [6] Y. Okada, Y. Tokumaru, *J. Appl. Phys.* 56 (1984) 314.
- [7] S. Hasegawa, K. Maehashi, H. Nakashima, T. Ito, A. Hiraki, *J. Cryst. Growth* 95 (1989) 113.
- [8] V. Levchenko, L. Postnova, V. Bondarenko, N. Vorozov, V. Yakovtseva, L. Dolgyi, *Thin Solid Films* 348 (1999) 141.
- [9] V. Yakovtseva, N. Vorozov, L. Dolgyi, V. Levchenko, L. Postnova, M. Balucani, V. Bondarenko, G. Lamedica, E. Ferrara, A. Ferrari, *Phys. Status Solidi A* 182 (2000) 195.
- [10] E.B. Chubenko, A.A. Klyshko, V.A. Petrovich, V.P. Bondarenko, *Thin Solid Films* 517 (2009) 5981.
- [11] V. Raiko, R. Spitzl, J. Engermann, V. Borisenko, V. Bondarenko, *Diamond Relat. Mater.* 5 (1996) 1063.
- [12] T. Yoshida, D. Komatsu, N. Shimokawa, H. Minoura, *Thin Solid Films* 451/452 (2004) 166.
- [13] K.-H. Li, C. Tsai, S. Shih, T. Hsu, D.L. Kwong, J.C. Campbell, *J. Appl. Phys.* 72 (1992) 3816.
- [14] J. Elias, R. Tena-Zaera, C. Lévy-Clément, *J. Electroanal. Chem.* 621 (2008) 171.
- [15] W.C. Zhang, X.L. Wu, H.T. Chen, J. Zhu, G.S. Huang, *J. Appl. Phys.* 103 (2008) 3718.
- [16] A. Janotti, C.G. Van de Walle, *Appl. Phys. Lett.* 87 (2005) 2102.
- [17] C.M. Mo, Y.H. Li, Y.S. Liu, Y. Zhang, L.D. Zhang, *J. Appl. Phys.* 83 (1998) 4389.